CRITICAL EVALUATION OF SMALL COMMERCIAL GAS CYLINDERS ANALYSIS

MTRL 585
Case Study 4

Prepared By:
GROUP 7

Janna Fabris
[redacted]

Wade Gubbels
[redacted]

Ibrahim Gadala
[redacted]

Darren Bromley
[redacted]

Submitted 6 November 2012

Contents

List of Figures

List of Tables

1.0 INTRODUCTION

Authors N. Davison and M.R. Edwards have presented a thorough analysis of potential failure modes of small gas cylinders to better understand the process and the potential danger [1]. The approach taken was recreated, and then critically evaluated to explore opportunities for improving the methods.

2.0 FACTS AND EVENTS

2.1 Background

Rather than analyzing an in-service failure, the authors analyzed performance and failure modes of pressure liquefied gas (PLG) cylinders. Of particular interest in PLG cylinders is the potential for boiling liquid expanding vapour explosion (BLEVE), which is a concern if a rapid pressure drop is encountered. An example was presented in which pressure of a gas cylinder was monitored while it was penetrated with a rifle bullet. Following the initial drop in pressure from its initial 27 bar, rapid vaporization of the PLG caused a subsequent pressure pulse up to 35 bar due to BLEVE.

The type of gas cylinder studied is expected to comply with British Standard BS EN 417:1992. Relevant details of the gas cylinders are as follows:

- Capacities ranging from 50 to 1000 mL
- Body of cylinder constructed of metal
- Maximum pressure of 12 bar at 50^{o}C
- Pressure tested at 10 bar, or 1.5 times the pressure created by the gas at 50^{o}C (whichever is greater)
- Pressure test shall not cause leakage or permanent deformation
- Leakage must not occur at pressures greater than 1.2 times the test pressure

Although the cylinders are not required to include pressure relief valves, those larger than 40 mm in diameter must have a concave base. In an over-pressure situation, the concave base is expected to invert, thus reducing the pressure. The pressure required to invert the base must be less than that which will cause leakage or permanent deformation of the body.

BLEVE failure of a PLG cylinder may result in blast, projectiles, and/or fireballs. Projectiles are considered the most far-reaching hazard from a BLEVE, which may include either large pieces of the container or nearby or attached objects. Study of prior BLEVE incidents reveals that less than 5 fragments should be expected, and 80% of fragments travel less than 200 m. The concave base separated from the body usually travels the furthest distance, and quite often, the remaining body stays intact as one large projectile. Research on such events (known as tub rockets) suggests that fragments would likely only cause non-penetrating blunt trauma injuries.

2.2 Cylinders Used

The cylinders used for this study contained 440 g liquefied mixture of 70% butane and 30% propane. They consisted of three parts: deep drawn body, concave base, and a type 1 threaded center valve cup. Following are some characteristics of the steel:

- Composition (wt.%): C = 0.028, Si = 0.002, Mn = 0.211, P = 0.012, S = 0.012, Cr = 0.019, Ni = 0.016, Al = 0.019, Cu = 0.028, Fe = balance
- Microstructure: predominantly ferrite, with small fraction pearlite, cold worked
- Hardness: Vickers 300 g load = 187 ± 3.8 (10 measurements)
- Average internal radius = 52.72 mm
- Average wall thickness = 0.38 mm

3.0 ENGINEERING ANALYSIS

3.1 Theoretical Analysis (Clausius-Clapeyron Governing Equation)

Governing Equation

The Clausius-Clapeyron equation is the governing equation that describes the pressure and temperature relationship at liquid-gas phase boundaries (equilibrium). This equation can be used to determine the coexistence curve for liquefied gases and is given by:

$$ln\left(\frac{P}{P_{ref}}\right) = \frac{\Delta H_{vap}}{R}\left(\frac{1}{T_{ref}} - \frac{1}{T}\right)$$

$$P = P_{ref}.e^{\frac{\Delta H_{vap}}{R}\left(\frac{1}{T_{ref}} - \frac{1}{T}\right)}$$

Where the following variables are:

P = vapour pressure
T = temperature
R = gas constant
ΔH_{vap} = latent heat of vaporization (enthalpy)

The enthalpy of vaporization is a gas specific property and, for many standard gases, can be obtained from chemistry handbooks. From reference [2] the following chemical properties are obtained for a 70% butane / 30% propane gas mixture.

Table 1: Chemical properties obtained from reference [2]

	P_{ref} [Pa]	T_{ref} [K]	ΔH_{vap} [J/mol]
Butane	101325 [=1 atm]	273	22440
Propane	101325	232	19040

Additionally, from reference [2] the gas constant is given by R = 8.3145 J/(mol K).

A rule of mixtures is used to determine the temperature-pressure relationship for the 70% butane / 30% propane gas mixture:

$$P_{70-30} = P_{ref}\left[0.7e^{\frac{\Delta H_{vap-but}}{R}\left(\frac{1}{T_{ref-but}}-\frac{1}{T}\right)} + 0.3e^{\frac{\Delta H_{vap-prop}}{R}\left(\frac{1}{T_{ref-prop}}-\frac{1}{T}\right)}\right]$$

$$P_{70-30} = 101325\left[0.7e^{\frac{22440}{8.3145}\left(\frac{1}{273}-\frac{1}{T}\right)} + 0.3e^{\frac{19040}{8.3145}\left(\frac{1}{232}-\frac{1}{T}\right)}\right]$$

For example, at 20°C (293K), the calculated vapour pressure of the mixed gas is:

$$P_{70-30_{293K}} = 101325\left[0.7e^{\frac{22440}{8.3145}\left(\frac{1}{273}-\frac{1}{293}\right)} + 0.3e^{\frac{19040}{8.3145}\left(\frac{1}{232}-\frac{1}{293}\right)}\right] = 0.38MPa$$

Thinned Walled Pressure Vessel Theory

Pressure vessels exhibit a three dimensional stress state. For thin-walled pressure vessels, this stress state is such that:

$$\sigma_h = 2\sigma_a, and\ \sigma_r \approx 0$$

Where:

σ_h = circumferential (hoop) stress
σ_a = axial (longitudinal) stress
σ_r = radial stress

Thus catastrophic rupture of the pressure vessel, manifesting in the formation of longitudinal cracks in the cylinder's wall, is expected to occur when the circumferential stress exceeds the vessel material's yield strength. The circumferential stress in a thin walled pressure vessel is given by:

$$\sigma_h = \frac{Pr}{t}$$

Where the following variables are:

P = internal pressure (obtained from the Clausius-Clapeyron equation)
r = pressure vessel radius
t = pressure vessel wall thickness

The authors specify the geometry of the canisters tested [1] as reported in Section 2.2.

Thus, for example, the calculated circumferential stress at 20°C (293K) is:

$$\sigma_{h_{293K}} = \frac{(0.38 \times 10^6) \times (52.72 \times 10^{-3})}{(0.38 \times 10^{-3})} = 53MPa$$

The theoretical coexistence curve for the 70% butane / 30% propane gas mixture can be determined, as shown in Figure 1 and Table 2. Additionally the measured ultimate strength of the canister material (estimated from the authors' article) is plotted. The temperature range of interest is from 20°C to 180°C.

Rather than plot this coexistence curve as a function of internal pressure versus temperature, the authors' chose to plot this curve as a function of circumferential stress versus temperature. Experimentally measured tensile strength is also shown as a function of temperature.

According to Figure 1, the intersection of this maximum circumferential stress and the ultimate tensile strength occurs approximately at 120°C (compared to 128°C as reported by the authors). This corresponds to a circumferential stress of 450MPa and an internal pressure of 3.25MPa (3.14 MPa as reported by the authors).

$$P_{70-30_{393K}} = \frac{(450 \times 10^6) \times (0.38 \times 10^{-3})}{(52.72 \times 10^{-3})} = 3.25MPa$$

Thus the canister is predicted to fail at approximately 3.25MPa.

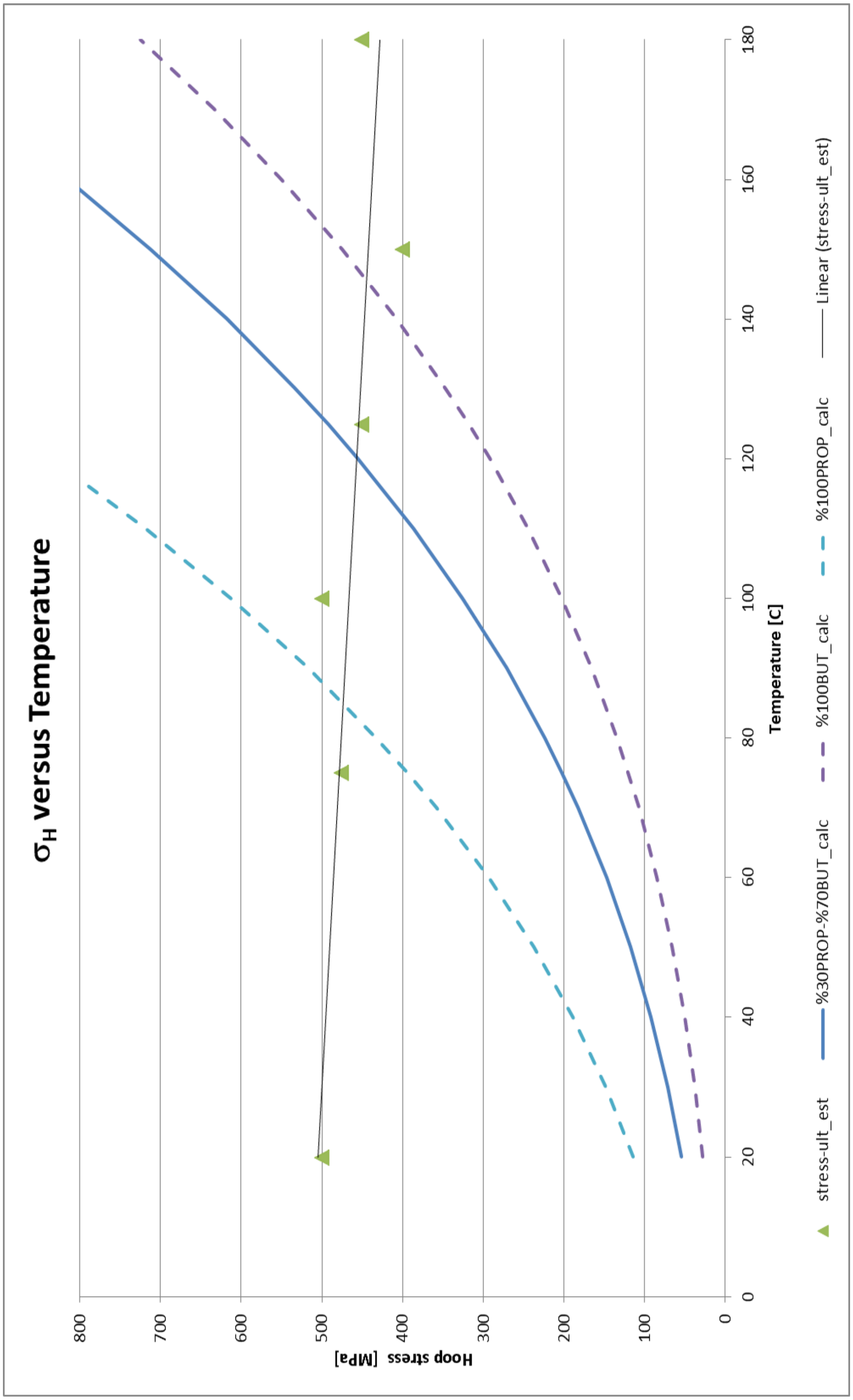

Figure 1: Circumferential (hoop) stress versus temperature (coexistence curve)

Table 2: Clausius-Clapeyron derived coexistence curve data-table

								%30PROP-%70BUT_calc	%100BUT_calc	%100PROP_calc		stress-ult_est
								[MPa]				[MPa]
T1 [C]	T1 [K]	0.7*$P1_{BUT}$	0.3*$P1_{PROP}$	P1	$P1_{BUT}$	$P1_{PROP}$		σ_H				σ_{UTS}
20	293	141724	248120	389844	202463	827066		**54**	28	115		500
30	303	192015	321049	513064	274308	1070163		**71**	38	148		
40	313	255156	408633	663789	364509	1362110		**92**	51	189		
50	323	333146	512403	845549	475923	1708011		**117**	66	237		
60	333	428064	633856	1061920	611521	2112853		**147**	85	293		
70	343	542049	774435	1316484	774355	2581450		**183**	107	358		
75	348	606868	852331	1459198	866954	2841102		**202**	120	394		475
80	353	677268	935519	1612787	967526	3118397		**224**	134	433		
90	363	835904	1118409	1954313	1194149	3728028		**271**	166	517		
100	373	1020125	1324317	2344442	1457322	4414390		**325**	202	612		500
110	383	1232071	1554363	2786434	1760101	5181210		**387**	244	719		
120	393	1473829	1809566	3283395	2105470	6031886		**456**	292	837		
125	398	1606524	1946891	3553415	2295034	6489637		**493**	318	900		450
130	403	1747425	2090841	3838265	2496321	6969469		**533**	346	967		
140	413	2054802	2398999	4453801	2935431	7996664		**618**	407	1109		
150	423	2397813	2734747	5132560	3425447	9115822		**712**	475	1265		400
160	433	2778210	3098685	5876894	3968871	10328950		**815**	551	1433		
170	443	3197632	3491314	6688946	4568046	11637713		**928**	634	1615		
180	453	3657607	3913034	7570641	5225153	13043448		**1050**	725	1810		450

3.2 Analysis of Kinetic Energy and Projectile Dynamics Post BLEVE

As mentioned in all the BLEVE occurrences the cold drawn portion of the canister disconnected from the bottom cup at the rolled seam. This geometry creates what is referred to as a tub rocket. The behavior of this rocket can be analyzed using the kinematic equations of motion. In this analysis the acceleration due to air drag is assumed to be zero. Therefore, the average velocity, collected from high speed video analysis, will be used in the projectile motion and energy equations. The authors' recorded and measured values of the tub rocket are listed in Table 3 below [1].

Table 3: Given values of tub rocket geometry and motion

Mass (g)	146
Diameter (mm)	106
Length (mm)	160
Average Velocity (m/s)	65

The maximum radius of travel the tub rocket can obtain with initial position on the ground is the scenario in which the nose is rotated 45 degrees from the horizontal. After breaking the initial velocity into its x and y components we can use the equation below to solve for the time of flight.

$$\Delta Y = v_{0_y} * t \pm .5 * a_y * t^2$$

Therefore, time of flight (t) = 9.37 seconds.

Where;
$\Delta Y = 0$
v_{0_y} = 65(m/s) * sin(45°) = 45.96 m/s
a_y = -9.81 m/s^2

Knowing the time of flight, the change in x position can be found using the equation above in the x direction and again assuming zero acceleration in this direction. The change in x is, therefore, 431 m. This result is the maximum distance the rocket can travel in the x direction and is in agreement with the authors' findings.

The authors state that a more realistic scenario would be a canister lying horizontally 1 m above the ground (reasonable height of a commercial grill). Using the previously mentioned technique and assuming zero initial velocity in the y direction, a time of flight until contacting the ground can be found (t = 0.45 s). This time is again used to solve for the distance traveled in the x direction. Therefore, using 65 m/s as the initial velocity in the x direction and t = 0.45s, the change in x is found to be 29.25 m. This value is also in agreement with the authors' value.

To understand the possible damage the projectile may inflict, energy values must be known.

$$KE = .5 * m * v^2$$

Using the above equation where:
m = mass = 146 g
v = 65 m/s

Therefore, the maximum kinetic energy of the projectile is 309 Joules.

4.0 CRITICAL EVALUATION

4.1 Relevance and appropriateness of facts and information presented

Background information
Discussion of PLG cylinders and the Clausius-Clapeyron relationship for equilibrium of two-state cylinder contents is definitely relevant and crucial for this study. The authors reference many studies regarding BLEVE in PLG cylinders and subsequent pressure profiles, fragmentation behavior and impact of fragments. The amount of this information would be appropriate only if the authors conducted the same type of analysis in their study. This was sometimes not that case, like in the pressure wave tests for example. In the tests the authors referenced, pressure transducers were used to accurately measure pressure fluctuations with respect to time, while, in the paper, the authors simply report that a "blast [overpressure] was felt in the safety car 20 m from the barbecue".

Material testing
Understanding the material microstructure and testing the mechanical properties of the material used is normally an essential step in a failure analysis. In the paper, the authors reported the composition and microstructure of the steel, the hardness values (for different temperatures), and tensile strengths (for different temperatures). Although generally important, the composition and microstructure of the steel is not of great relevance in this specific case study. It may have been more appropriate if chemical interactions, such as corrosion, were involved, or if a change in microstructure was reported after exposure to the heat. Neither of these two points was qualitatively present in the paper, nor were any images of microstructure provided.

The appropriateness of the tensile strength values is questionable, since they were taken from the body of the canister. If the failure was due to stress in the hoop direction, it would be relevant, but this is not the case. Thus, it would have been more appropriate to quantify properties at the seam. A reasonable approach may be to perform microhardness tests in various locations of the seam, which can be correlated to the strength of the material with reasonable confidence. A comparison between microhardness of the body versus at the seam may also allow the authors to confirm or deny that the seam will have similar tensile properties as the body.

Another consideration is that the samples removed for tensile testing were presumably flattened. The additional cold work may affect the measured properties, and is prohibited by most tensile test standards.

Range and impact calculations
Judging from typical small gas cylinder usage, where the user is quite close to the can (< 1 m), the relevance of the range calculations presented by the authors is debatable. The authors claim that "it is important to be able to estimate the range of such cylinders", without giving one practical example as to how this is relevant to a typical user who will be standing very close to his/her barbeque and adjacent small gas cylinder can. Furthermore, the authors admit that the most realistic and feasible stacking orientation for the cans is vertically or horizontally, yet report calculations for the can at 45°. This was deemed irrelevant, since it is already known that a 45° starting angle gives the longest range (assuming no air resistance), and the typical user will most likely be much closer to the can than the range values calculated.

Our group also questioned the appropriateness of the impact comparison table 3. It is indeed useful to conclude that people within close proximity of a BLEVE of a small gas cylinder will experience blunt trauma injuries and not penetration injuries. However, extensive comparison to different rubber bullet types is not needed to reach this conclusion. Furthermore, rubber bullets are usually fired from medium to long range, while a typical user proximity to a gas cylinder during barbequing would be extremely close.

4.2 Missing information

Initial visual inspection
A useful step in failure analysis is to inspect components or structures before subjecting them to tests of any kind. This inspection can be with the naked eye or under magnification, and serves to identify and locate any flaws or areas of potential problems. In this case, a visual inspection of the critical seam location could have identified cracks, excessive plastic deformation or even changes in mechanical properties (using micro hardness indentation test for example), all which could have aided in the explanation of the seam failure mechanism. More simply, observations of how the seam was made (e.g. crimped, multiple rolls, etc.) would have provided useful information about the possible stress state in this critical area.

Inspection and material testing after failure
Assessment of fracture surfaces after failure testing can answer questions regarding the failure mechanism (brittle or ductile) and whether there were internal cracks or flaws in the structure. The reader would benefit in learning whether the seam tore

or simply unfolded. Other useful information can be addressed also, such as the presence and severity of environmental degradation, rate of fatigue growth (if present), and material hardness. In this specific case, the authors could have gained more understanding of the failure mechanism at the seam and the limiting material properties at failure by performing a fractographic assessment of the failure surface.

Sharp fragment assessment

The authors mentioned that secondary projectiles (nearby or attached objects like pipes, equipment etc.) are not considered. However, it is also mentioned that ductile failures (expected due to high temperatures) usually produce less than 5 projectiles, and do not always produce only two projectiles. Other than the two primary projectiles of tub-rocket type failures (base and can), other fragments can be sharp, as opposed to blunt, and can cause penetration of the human body. This is not investigated in detail although other, less important features of the projectiles are. Classification of fragments into only "fast" and "slow" categories disregards the fact that fragmentation from ductile failures, although slower than brittle failures, can also be sharp. Thus, information of more than two fragments during the failure tests has the potential of invalidating the authors' conclusion regarding blunt trauma injuries.

Velocity measurement method

The range and impact calculations presented by the authors depend strongly on the measured velocity of the tub-rocket after BLEVE. The method for this crucial measurement and its level of accuracy are not mentioned in the paper. This is important and should have been indicated, since even a 10-15% difference in this velocity measurement can significantly alter the impact and range results reported (kinetic energy is exponentially proportional to velocity). Velocity can be easily verified using analysis of high speed video footage.

4.3 Appropriateness of analysis presented

Correctness of high temperature testing setup

In the paper, high temperature tests are used to create high pressures and subsequently cause failure in the weakest location in the small cylinder test cylinder. The governing principles which these tests aim to simulate are valid, namely the increase of pressure with increased temperature and the possibility of a BLEVE due to a sudden large loss in pressure from a rupture.

The test setup used in the paper to create the failure scenario outlined above is described ambiguously. The paper states that "the cartridges were exposed to the heat from a small disposable barbeque whilst the wall temperatures (next to and 180° from the heat) were recorded via a set of K-thermocouples, one on the bottom and the other on the top at 180° from the bottom". This could equally describe the following 3 situations, where *a* represents the bottom thermocouple and *b* represents the top thermocouple:

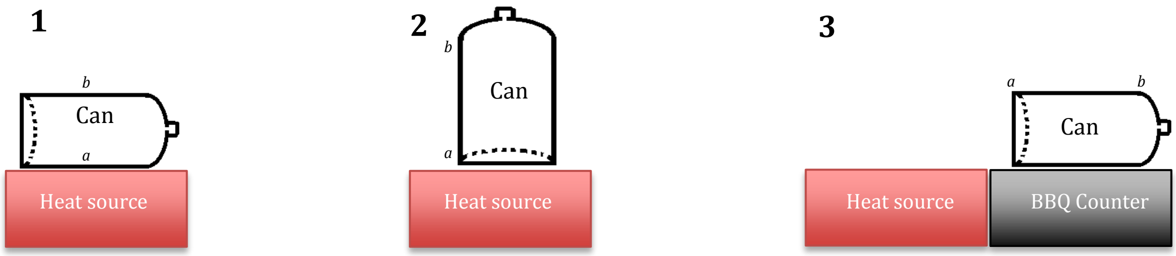

Figure 2: Possible canister orientations during high temperature tests

A detailed schematic or even a photograph showing the test setup should have been provided to avoid confusion and to enable proper analysis. Regardless of which setup of the 3 illustrated above the authors used, we believe unwanted factors are introduced into the failure by using a disposable BBQ as the heat source. The most important of these unwanted factors is the thermal stress in the wall material due the temperature gradient of the can. This can be quite significant, depending on the thermal gradient present and orientation of the container.

Another unwanted factor is different material strength in different parts of the can due to a temperature gradient in the can material. The authors predicted that there is no reduction in hardness and strength likely to occur due to the heat source, yet did not discuss this quantitatively.

Temperature gradients (and associated gradients in strength) and thermal stresses may have been avoided. If a uniform temperature environment was created around the can, such as from a convection oven, results would have been more consistent and useful. Although the test setup would be slightly more complicated, the results would likely be much more repeatable and dependable.

Test 4 (no BLEVE)

The authors reported a test case where no BLEVE occurred (test 4). Reasoning or explanation of why this specific test did not produce BLEVE was not given. Comparing the peak temperatures of the test 4 bottom thermocouple to other tests reveals that the bottom thermocouple temperature only reached 92° in test 4, but reached above 100° in two other tests that produced BLEVE. We believe this is probably the reason why no BLEVE occurred, as the resulting pressure might have not been enough to cause rupturing at the seam. There is a possibility that the can ruptured stably causing slow leaking, which was in turn not enough to cause a rapid pressure drop for BLEVE.

Surprisingly, the authors report another test (test 1) with a peak bottom thermocouple temperature of 92° which created a BLEVE. However, it was mentioned that test 4 took approximately 30 minutes more to heat up than test 1. It is not understood why it takes a significantly longer time to heat up the can in test 4 as opposed to the other tests. We believe the root cause of this outlying test 4 result is the inappropriate testing setup which rendered the investigators incapable of creating a consistent temperature profile for all the tests. Temperatures well over 100°C should be easy to recreate with a small barbeque. The data from test 4 provides no further information, and did not need to be reported.

Rolled seam

The small gas cylinder used in this study is assembled from three pieces: a deep drawn body, a concave base, and a threaded center valve cup. The critical location where all failures occurred during testing is the rolled seam joining the base and the main deep-drawn body. Judging from the importance of this location, an analysis of the local stresses should have been performed. It was observed that the direction of the crack at the seam was in the circumferential direction, meaning the stress causing growth is most probably in the axial direction of the can (normal to the crack length). Since the hoop stress is twice the value of the axial stress in thin-walled pressure vessels, significant residual stresses and possibly stress concentrations caused the effective axial stress to become larger than the hoop stress in this case. This is due to the rolling process used to manufacture the seam. Although it is difficult to quantify the stresses involved from this joining method analytically, the authors could have employed basic hand calculations (e.g. estimating the deflection/compression of outer/inner material during rolling, respectively) or numerical techniques (e.g. FEA) to analyze the seam location.

4.4 Failure prevention

Seam Rupture

It has been clearly demonstrated that the weak point of the canister is the rolled seam at the bottom. Unfortunately, the reason for failure at this location was not evaluated, so it is difficult to recommend an improvement. It is likely that a rolled seam is the cheapest processing option, so no change is required if all performance criteria are met. If a manufacturer wishes to prevent dangerous failures in cases where the canister is being used beyond its specified operating parameters, they may wish to consider a welded seam. Since axial stresses that caused failure of the seam are half the expected hoop stress, it may be beneficial to avoid potential stress concentrations or complex stress states associated with a rolled seam.

Burst Disk

Although not required by the standard, a common device used to prevent rupture due to over pressurization is a burst disk. The disk is designed to burst at a pressure slightly lower than the rupture pressure of the canister. With a controlled orifice size, the canister can vent itself without initiating a BLEVE event. Figure 3 shows an example of small size burst disks, in both ruptured (left) and intact (right) states.

Figure 3: Burst disks for over-pressure protection; ruptured (left) and intact (right)

4.5 General comments

The authors' analysis did not examine why the inversion of the base did not prevent BLEVE during the high temperature tests. This is a very important difference from the results of hydrostatic testing, which is likely due to changing too many control variables. For instance, using water versus PLG may play a role. Also, the equilibrium ratio of gas to liquid was not quantified and will determine the energy release during inversion of the base and rupture.

5.0 CONCLUSION

Key analytical theories employed by N. Davison and M.R. Edwards were recreated as part of this critical evaluation, including:

- Clausius-Clapeyron relationship of the pressure and temperature at liquid-gas phase boundaries
- Stress analysis of thin walled cylinder experiencing increased pressure
- Analysis of kinetic energy and projectile dynamics following a BLEVE event

The research and testing conducted was considered thorough, but still has potential for improvement. Following are the criticisms and recommendations than can be offered for the analysis:

- The analysis focused more on the potential failure in the body rather than the actual failure of the seam
- The authors did not investigate the reason for failure at the seam, even though it is clear they expected failure in the body due to hoop stress
- Assessing injury caused by a projectile at far distances seems irrelevant when operators will likely be very near to the canister (<1 m)
- High temperature tests could have used a more even heating method in order to obtain repeatable results

REFERENCES

[1] Davidson, N. and Edwards, M. R. "Effects of fire on small commercial gas cylinders". Engineering Failure Analysis 15 (2008) 1000-1008.

[2] CRC Handbook of Chemistry and Physics, 93rd edition (http://www.hbcpnetbase.com//articles/06_25_92.pdf), downloaded Oct 18th 2012